An efficient and accurate approximation to time-dependent density functional theory for systems of weakly coupled monomers

Jie Liu and John M. Herbert[a)]
Department of Chemistry and Biochemistry, The Ohio State University, Columbus, Ohio 43210, USA

(Received 12 May 2015; accepted 3 July 2015; published online 17 July 2015)

A novel formulation of time-dependent density functional theory (TDDFT) is derived, based on non-orthogonal, absolutely-localized molecular orbitals (ALMOs). We call this approach TDDFT(MI), in reference to ALMO-based methods for describing molecular interactions (MI) that have been developed for ground-state applications. TDDFT(MI) is intended for efficient excited-state calculations in systems composed of multiple, weakly interacting chromophores. The efficiency is based upon (1) a local excitation approximation; (2) monomer-based, singly-excited basis states; (3) an efficient localization procedure; and (4) a one-step Davidson method to solve the TDDFT(MI) working equation. We apply this methodology to study molecular dimers, water clusters, solvated chromophores, and aggregates of naphthalene diimide that form the building blocks of self-assembling organic nanotubes. Absolute errors of 0.1–0.3 eV with respect to supersystem methods are achievable for these systems, especially for cases involving an excited chromophore that is weakly coupled to several explicit solvent molecules. Excited-state calculations in an aggregate of nine naphthalene diimide monomers are ~40 times faster than traditional TDDFT calculations. [http://dx.doi.org/10.1063/1.4926837]

I. INTRODUCTION

Studies of excited electronic states in the condensed phase must carefully balance accuracy against computational efficiency, and time-dependent density functional theory[1–5] (TDDFT) is therefore the workhorse method for computing excitation energies of low-lying excited states.[4–8] Nevertheless, the computational cost of standard TDDFT scales as $O(N^4)$ with system size, or $O(N^3)$ with density fitting,[9] which becomes prohibitive for large systems such as the photosynthetic light harvesting system or organic semiconductors with interesting energy-transfer properties, or when numerous explicit solvent molecules are included, in order to converge a solution-phase excitation energy. For such applications, further approximations and linear-scaling algorithms must be developed even to apply TDDFT.

Various approximations that exploit locality have been proposed in order to speed up TDDFT calculations and eventually realize $O(N)$ scaling.[10] These include atomic orbital (AO) implementations by Baerends *et al.*[9] and by Helgaker *et al.*[11,12] that achieve linear scaling by use of pre-screening techniques and sparse matrix algebra. TDDFT within the frozen-density embedding framework was developed by Casida and Wesołowski[13] and uses well-defined, localized fragment densities to achieve linear scaling. Neugebauer and co-workers later extended this method.[14,15] Chen *et al.*[16] developed a linear-scaling TDDFT method using the localized density matrix in an orthogonal AO representation, which Yang *et al.*[17] later extended to use non-orthogonal localized molecular orbitals (LMOs). Liu *et al.*[18] derived LMOs from capped fragment canonical MOs and used them to realize a linear-scaling TDDFT method. Local approximations in TDDFT are conceptually attractive for weakly interacting systems where the excitations are usually localized on a small active region.

In contrast, there exist a broad class of weakly interacting molecular complexes whose excited states may exhibit "excitonic" delocalization,[19,20] including liquids (and solution-phase chromophores), molecular aggregates, and even proteins. Intermolecular interactions in these complexes result not only in spectral shifts but also can give rise to interesting excited-state properties that are potentially very different from those of a single chromophore. Examples include hydrogen-bonding interactions that facilitate fluorescence quenching,[21,22] or the excitonic delocalization engendered by Coulomb couplings between multiple chromophores.[19,20,23,24] There is, therefore, considerable interest in developing low-cost theoretical approaches for describing electronically excited states in ensembles of weakly interacting molecules.

For weakly interacting complexes, a popular and very old theoretical model of exciton delocalization is the Frenkel-Davydov exciton model,[19,20] which is an absolutely-localized strategy. In its original, long-ago formulation,[25,26] this model assumed dipole couplings between chromophores and could therefore be expected to work well only if the charge distributions of the individual chromophores were well separated, or at least non-overlapping. This version of the model still sees application in contemporary times, e.g., for H- and J-aggregates[27,28] or the photosynthetic light-harvesting complex,[29] but its generality is lacking. While specific parameters in the model, namely, monomeric excitation energies and Coulomb couplings between transition densities, can be efficiently calculated using TDDFT, electronic overlap and

a)herbert@chemistry.ohio-state.edu

exchange effects are typically neglected, which is problematic at short range.

Recently, several *ab initio* exciton models that include both Coulomb and exchange coupling have been put forward as promising alternatives to the traditional Frenkel-Davydov model.[20,30] These methods employ a fragment-based approach for efficiency, yet without the dipole-coupling approximation of older approaches. Inspired by this work, we propose herein a new TDDFT strategy based on non-orthogonal, absolutely-localized molecular orbitals (ALMOs), which have recently seen use for ground-state calculations of intermolecular interactions.[31–33] [An extension to excited states at the level of configuration interaction singles (CIS) is also in progress.[34]] We assume that the AO basis consists of atom-centered functions, and "absolute" localization means that only AO basis functions centered on a given monomer are allowed to contribute to that monomer's MOs. In our approach, absolutely-localized excitations on individual monomers are computed in an "embarrassingly parallel" fashion, then coupled together to describe excited states of the supersystem.

The equation of motion for the time-dependent ALMOs that is derived herein turns out to be the same as in the non-orthogonal LMO treatment of Yang *et al.*[17] Those authors pursued a time-domain approach, which can be advantageous in large systems where numerous excited states are desired, because it does not require propagation of virtual orbitals and therefore sidesteps a significant memory bottleneck in the more traditional frequency-domain approach, at the expense of a large increase in computer time.

In contrast, we will derive a linear-response (LR) method in the frequency domain, which is advantageous when the number of desired states is small, as in the case of a well-defined chromophore that is weakly coupled to a number of explicit solvent molecules. (However, we will test this method in difficult cases where the system consists of identical chromophores, in order to explore its possible limitations.) Two approximation will be applied in the numerical implementation: (i) the orthogonality between the occupied space and the virtual space will be discarded in order to better retain the localized character of the method and (ii) excitations are restricted to be localized on the absolutely-localized fragments, with no explicit charge transfer between different fragments. The environmental effect therefore enters the calculation in two ways: first, via changes in the orbitals and orbital energies that are polarized by their environment (which one suspects is often the dominant contribution),[35] and second, in terms of explicit couplings between monomer basis states, as in the excitonic formalism.

When only a few low-lying excited states are desired, the conventional, frequency-domain TDDFT equations (Casida equations[1]) are usually solved via Davidson iteration.[36,37] The number of iterations required to reach convergence varies with the system and with the number of desired eigenvalues, but 10–30 iterations is typical when several (but $\ll 30$) eigenvalues are requested and simple occupied → virtual initial guesses are employed for the trial vectors. In the case of a local approximation using ALMOs, however, a very good initial guess can be extracted from the fragment excited states. As a result, we will show that the iterative solution of the ALMO-TDDFT eigenvalue problem for the supersystem can be approximated by a one-step diagonalization in the subspace of trial vectors, without significant loss of accuracy. In order to construct the ALMO-TDDFT eigenvalue equation in the trial vector subspace, it is necessary to calculate the supersystem Fock matrix and $N_{\text{fragment}} \times N_{\text{fragment}}$ coupling matrix, which requires about the same effort as two calculations of all two-electron integrals for the supersystem. This leads to a dramatic reduction in computational time.

II. THEORY

A. Overview

The idea of computing excited states of individual chromophores independently, then coupling them together in a separate step, has obvious appeal.[20] A disadvantage is that the ALMOs on each chromophore are non-orthogonal. In the usual formulation of LR-TDDFT, the density response is truncated at first order, and the zero-order condition is simply the self-consistent field (SCF) convergence condition. Stoll *et al.*[38] were the first to write down an SCF equation in the ALMO basis, and Nagata *et al.*[39] proposed to refer to such methods (originally developed for ground-state SCF calculations) as a *locally projected self-consistent field for molecular interactions* (MI). Such methods have been modified for practical calculations by Head-Gordon and co-workers,[31] who refer to the method as SCF(MI). We shall follow the latter notation for our ALMO-based excited-state methods, which we term TDDFT(MI), or TDA(MI) when the Tamm-Dancoff approximation[40] (TDA) is invoked, or CIS(MI) for CIS calculations in the ALMO basis.

Liu *et al.*[18] have argued that there exist two types of locality in TDDFT—in energy and in space—and that a good $O(N)$ algorithm must balance these two localities. Canonical MOs tend to be delocalized throughout the system, such that the Coulomb and the exchange(-correlation) terms between MOs cannot easily be truncated using any pre-defined condition. As such, the canonical MO representation may be considered to be local in energy (since the MOs have well-defined one-particle energies) but delocalized in space. On the other hand, the AOs are "local in space but delocalized in energy,"[18] such that the Hamiltonian in the AO representation is extremely dense (as compared to that in the MO representation), leading to late-crossover $O(N)$ methods. LMOs offer a good balance, being somewhat localized in both energy and in space. For the TDDFT(MI) method developed below, it is found that the energy is blocked-localized in the sense that the Hamiltonian is block-diagonal in the fragment MO representation, yet at the same time the ALMOs are spatially localized on fragments.

In this paper, we will combine TDDFT with the SCF(MI) method and thereby propose a new linear-scaling TDDFT method to treat molecular excited states in the condensed phase. Section II B below provides a brief summary of how TDDFT is formulated for non-orthogonal LMOs. Then, in Section II C, we extend ALMO-TDDFT into the frequency domain to obtain TDDFT(MI) working equations, which we further simplify by means of several additional approximations:

1. a local excitation approximation;
2. an efficient localization method;
3. the Tamm-Dancoff approximation;[40] and
4. a one-step Davidson solution for the eigenvalues.

Numerical results are presented in Section III and conclusions appear in Section IV.

B. TDDFT with non-orthogonal MOs

In this section, we first introduce the equation of motion for non-orthogonal MOs. Indices $i,j,k,\ldots$ label occupied MOs; $a,b,\ldots$ label virtual MOs; $p,q,r,\ldots$ label arbitrary MOs; and $\mu,\nu,\ldots$ label AOs.

The equation of motion for the one-particle density operator, $\hat{\rho}$, that is constructed from the Kohn-Sham determinant is

$$i\frac{\partial\hat{\rho}(r,t)}{\partial t} = [\hat{f},\ \hat{\rho}(r,t)], \tag{1}$$

where $\hat{f}$ is the Kohn-Sham effective Hamiltonian,

$$\hat{f}[\hat{\rho}(r,t)](t) = -\tfrac{1}{2}\hat{\nabla}^2 + \hat{V}_{\rm ext}(r,t) + \int \frac{\hat{\rho}(r',t)}{|r-r'|}\,dr' + \hat{V}_{\rm xc}(r,t). \tag{2}$$

The quantity

$$\hat{V}_{\rm xc}(r,t) = \frac{\delta E_{\rm xc}}{\delta\hat{\rho}(r,t)} \tag{3}$$

is the exchange-correlation potential. If the molecular orbitals are orthogonal, then Casida's non-Hermitian eigenvalue equation[1] can be derived from Eq. (1), or alternatively the one-particle density operator can be propagated in real time.[41] For simplicity, the variables (r,t) will be dropped hereafter. Note that Eq. (3) tacitly invokes the adiabatic approximation[1] (which we assume throughout), in the sense that $\hat{V}_{\rm xc}$ contains no memory or retardation effects.

In the non-orthogonal MO representation, the one-particle density operator is

$$\hat{\rho} = \sum_{ij}^{N} |\phi_i\rangle S^{-1}_{ij}\langle\phi_j|, \tag{4}$$

where $S_{ij} = \langle\phi_i|\phi_j\rangle$ is an overlap matrix element. It is easy to demonstrate that $\hat{\rho}$ satisfies the following conditions:

$$\hat{\rho}\hat{\rho} = \hat{\rho}, \tag{5a}$$
$$\hat{\rho}^\dagger = \hat{\rho}, \tag{5b}$$
$$\mathrm{tr}\hat{\rho} = N. \tag{5c}$$

From Eq. (4),

$$\frac{\partial\hat{\rho}}{\partial t} = \sum_{ij}^{N}\left[\left(\frac{\partial|\phi_i\rangle}{\partial t}\right)S^{-1}_{ij}\langle\phi_j| + |\phi_i\rangle\left(\frac{\partial S^{-1}_{ij}}{\partial t}\right)\langle\phi_j| + |\phi_i\rangle S^{-1}_{ij}\left(\frac{\partial\langle\phi_j|}{\partial t}\right)\right]. \tag{6}$$

Since $\mathbf{S}\mathbf{S}^{-1} = \mathbf{1}$, we have

$$\frac{\partial\mathbf{S}^{-1}}{\partial t} = -\mathbf{S}^{-1}\left(\frac{\partial\mathbf{S}}{\partial t}\right)\mathbf{S}^{-1}. \tag{7}$$

Inserting Eqs. (6) and (7) into Eq. (1), and following some rearrangement, one obtains

$$\begin{aligned}\frac{\partial\hat{\rho}}{\partial t} &= (1-\hat{\rho})\sum_{ij}^{N}\left(\frac{\partial|\phi_i\rangle}{\partial t}\right)S^{-1}_{ij}\langle\phi_j| \\ &\quad + \sum_{ij}^{N}|\phi_i\rangle S^{-1}_{ij}\left(\frac{\partial\langle\phi_j|}{\partial t}\right)(1-\hat{\rho}) \\ &= i[\hat{\rho},\ \hat{f}\,].\end{aligned} \tag{8}$$

C. LR-TDDFT with non-orthogonal MOs

The first-order response of the MOs, the density, and the Fock operator with respect to an external perturbation can be expressed formally as

$$\phi = \phi_0 + \lambda\ \delta\phi + O(\lambda^2), \tag{9a}$$
$$\hat{\rho} = \hat{\rho}_0 + \lambda\ \delta\hat{\rho} + O(\lambda^2), \tag{9b}$$
$$\hat{f} = \hat{f}_0 + \lambda\ \delta\hat{f} + O(\lambda^2). \tag{9c}$$

The zeroth-order condition, from Eq. (8), is

$$[\hat{f}_0,\ \hat{\rho}_0] = 0, \tag{10}$$

which is simply the ground-state SCF convergence condition. The first-order response equation can be extracted from Eq. (8) as well, and it is

$$\begin{aligned}i(1-\hat{\rho}_0)\sum_{ij}^{N}\left(\frac{\partial\delta|\phi_i\rangle}{\partial t}\right)S^{-1}_{0,ij}\langle\phi_{0,j}| \\ + i\sum_{ij}^{N}|\phi_{0,i}\rangle S^{-1}_{0,ij}\left(\frac{\partial\delta\langle\phi_j|}{\partial t}\right)(1-\hat{\rho}_0) \\ = [\hat{f}_0,\ \delta\hat{\rho}] + [\delta\hat{f},\ \hat{\rho}_0].\end{aligned} \tag{11}$$

The notation $\phi_{0,p}$ indicates a ground-state MO, and $\mathbf{S}_0$ is the overlap matrix between ground-state MOs. Hereafter, we will drop the zero subscripts and let ϕ_p and $\mathbf{S}$ represent ground-state MO and overlap matrix, respectively. The quantity $\delta\hat{f}$ is the coupling matrix, whose AO matrix elements are

$$\begin{aligned}\delta f_{\mu\nu\sigma}[\delta\rho] = \sum_{\kappa\lambda\sigma'}\big[&(\mu\nu\sigma|\kappa\lambda\sigma') - C_{\rm x}(\mu\lambda\sigma|\kappa\nu\sigma') \\ &+ f^{xc}_{\mu\nu\sigma,\kappa\lambda\sigma'}\big]\delta\rho_{\kappa\lambda\sigma'},\end{aligned} \tag{12}$$

where $C_{\rm x}$ is the coefficient of Hartree-Fock exchange, in the case of a hybrid functional, and σ is a spin index.

Multiplying Eq. (11) by $(1-\hat{\rho}_0)$ from the left and by $\hat{\rho}_0$ from the right, one obtains

$$\begin{aligned}i(1-\hat{\rho}_0)\sum_{ij}^{N}\left(\frac{\partial\delta|\phi_i\rangle}{\partial t}\right)S^{-1}_{ij}\langle\phi_j| \\ = (1-\hat{\rho}_0)[\hat{f}_0,\ \delta\hat{\rho}]\hat{\rho}_0 + (1-\hat{\rho}_0)[\delta\hat{f},\ \hat{\rho}_0]\hat{\rho}_0,\end{aligned} \tag{13}$$

where the following relations have been used:

$$\hat{\rho}_0|\phi_i\rangle = |\phi_i\rangle, \tag{14a}$$
$$\hat{\rho}_0(1-\hat{\rho}_0) = 0. \tag{14b}$$

Alternatively, multiplying Eq. (11) by $(1-\hat{\rho}_0)$ from the right and by $\hat{\rho}_0$ from the left, one obtains

$$i\sum_{ij}^{N}|\phi_i\rangle S_{ij}^{-1}\left(\frac{\partial\delta\langle\phi_j|}{\partial t}\right)(1-\hat{\rho}_0) = \hat{\rho}_0[\hat{f}_0,\,\delta\hat{\rho}](1-\hat{\rho}_0)+\hat{\rho}_0[\delta\hat{f},\,\hat{\rho}_0](1-\hat{\rho}_0). \quad (15)$$

Transforming Eqs. (13) and (15) into the frequency domain, we have

$$\omega(1-\hat{\rho}_0)\sum_{ij}^{N}|\delta\phi_i(\omega)\rangle S_{ij}^{-1}\langle\phi_j| = (1-\hat{\rho}_0)[\hat{f}_0,\,\delta\hat{\rho}]\hat{\rho}_0+(1-\hat{\rho}_0)[\delta\hat{f},\,\hat{\rho}_0]\hat{\rho}_0 \quad (16)$$

and

$$\omega\sum_{ij}^{N}|\phi_i\rangle S_{ij}^{-1}\langle\delta\phi_j(\omega)|(1-\hat{\rho}_0) = \hat{\rho}_0[\hat{f}_0,\,\delta\hat{\rho}](1-\hat{\rho}_0)+\hat{\rho}_0[\delta\hat{f},\,\hat{\rho}_0](1-\hat{\rho}_0). \quad (17)$$

Next, expand the first-order response in the basis of unperturbed MOs,

$$\delta|\phi_i\rangle = \sum_{ai}X_{ai}|\phi_a\rangle, \quad (18a)$$

$$\delta\langle\phi_i| = \sum_{ai}Y_{ai}\langle\phi_a|. \quad (18b)$$

This leads to expressions for the matrix elements of the transition densities,

$$\delta\hat{\rho}_{ai} = X_{ai}\sum_{j}(1-\hat{\rho}_0)|\phi_a\rangle S_{ij}^{-1}\langle\phi_j|, \quad (19a)$$

$$\delta\hat{\rho}_{ia} = Y_{ai}\sum_{j}S_{ij}^{-1}|\phi_j\rangle\langle\phi_a|(1-\hat{\rho}_0). \quad (19b)$$

Now we define new MOs

$$\widetilde{\phi}_i = \sum_j \phi_j S_{ij}^{-1} \quad (20)$$

and

$$\widetilde{\phi}_a = (1-\hat{\rho}_0)\phi_a. \quad (21)$$

In this new MO basis, the transition density is simpler,

$$\delta\hat{\rho}_{ai} = X_{ai}|\widetilde{\phi}_a\rangle\langle\widetilde{\phi}_i|, \qquad \delta\hat{\rho}_{ia} = Y_{ai}|\widetilde{\phi}_i\rangle\langle\widetilde{\phi}_a|. \quad (22)$$

Rewriting Eqs. (16) and (17) in the new non-orthogonal MO representation of Eqs. (20) and (21), one obtains after some rearrangement

$$\begin{pmatrix}\widetilde{\mathbf{A}} & \widetilde{\mathbf{B}}\\ \widetilde{\mathbf{B}} & \widetilde{\mathbf{A}}\end{pmatrix}\begin{pmatrix}\mathbf{X}\\ \mathbf{Y}\end{pmatrix} = \omega\begin{pmatrix}\widetilde{\mathbf{\Delta}} & \mathbf{0}\\ \mathbf{0} & -\widetilde{\mathbf{\Delta}}\end{pmatrix}\begin{pmatrix}\mathbf{X}\\ \mathbf{Y}\end{pmatrix}. \quad (23)$$

Matrix elements in non-orthogonal "tilde" representation are

$$\widetilde{A}_{ai\sigma,bj\sigma'} = \widetilde{f}_{ab}\widetilde{S}_{ij}\delta_{\sigma\sigma'}-\widetilde{f}_{ij}\widetilde{S}_{ab}\delta_{\sigma\sigma'}+(\widetilde{a}_\sigma\widetilde{i}_\sigma|\widetilde{b}_{\sigma'}\widetilde{j}_{\sigma'}) - C_{\rm x}\delta_{\sigma\sigma'}(\widetilde{a}_\sigma\widetilde{b}_\sigma|\widetilde{i}_{\sigma'}\widetilde{j}_{\sigma'})+\widetilde{f}^{\rm xc}_{ai\sigma,bj\sigma'}, \quad (24)$$

$$\widetilde{B}_{ai\sigma,bj\sigma'} = (\widetilde{a}_\sigma\widetilde{i}_\sigma|\widetilde{b}_{\sigma'}\widetilde{j}_{\sigma'})-C_{\rm x}\delta_{\sigma\sigma'}(\widetilde{a}_\sigma\widetilde{j}_\sigma|\widetilde{b}_{\sigma'}\widetilde{i}_{\sigma'}) +\widetilde{f}^{\rm xc}_{ai\sigma,bj\sigma'}, \quad (25)$$

$$\widetilde{\Delta}_{ai\sigma,bj\sigma'} = \widetilde{S}_{ab}\widetilde{S}_{ij}\delta_{\sigma\sigma'}. \quad (26)$$

D. Local approximation to ALMO-TDDFT

In cases of weakly interacting subsystems, it is not necessary to solve Eq. (23) in whole *occ* ⊗ *vir* space although it may be possible to achieve linear scaling by use of screening techniques and sparse-matrix algebra. Alternatively, if the electronic transitions occur in a small active region of the supersystem, or can be described as linear combinations of such localized excitations, then a local approximation in TDDFT may be very efficient and accurate.

In the local approximation, the total electronic excitation is expressed as a linear combination of localized excitations between localized ground-state MOs. Compared with the LMO representations proposed in other $O(N)$ TDDFT methods, the ALMOs used in this work are *absolutely* localized, which we have defined rigorously above but which operationally means that they are largely free of the "orthogonalization tails" that often appear upon orbital localization. The ALMOs thus preserve some locality in both space and energy. Stoll's SCF(MI) method[31,38] is used to compute the ground-state ALMOs.

1. Absolutely local excitation approximation

In the ALMO representation, the TDDFT working equation [Eq. (23)] is based on molecular orbitals expanded in local subsets of AOs. Equation (23) contains, in addition to local excitation terms, numerous charge-transfer terms whose omission greatly reduces the number of variables required to describe the supersystem transition densities. We omit these charge-transfer terms in our TDDFT(MI) method, since the dominant excitations in weakly interacting systems are the local ones. For a more strongly interacting system, such as a water cluster, part of the short-range interactions are included in TDDFT(MI) by retaining some overlap between the occupied space and the virtual space, as discussed below (Section II D 2).

Omitting the explicit charge transfer terms and thus confining the excitations within monomer units, which we label below by x and y $(=1,2,\ldots,N_{\rm fragment})$, the total transition density can be expanded in monomer excited states,

$$\delta\rho_{\rm total} = \sum_{x}^{N_{\rm fragment}}\sum_{m\subset x}^{N_{\rm roots}}U_{x,m}\,\delta\rho_{x,m}. \quad (27)$$

Here, $N_{\rm roots}$ is the number of monomer excited states that are chosen. Despite the notation that is adopted in Eq. (27), there is no requirement that the same number of roots be used for each monomer. The TDDFT(MI) working equation can be written as

$$\frac{1}{2}\sum_{y,n}\Big[(\mathbf{X}+\mathbf{Y})^\dagger_{x,m}(\mathbf{A}+\mathbf{B})(\mathbf{X}+\mathbf{Y})_{y,n} + (\mathbf{X}-\mathbf{Y})^\dagger_{x,m}(\mathbf{A}-\mathbf{B})(\mathbf{X}-\mathbf{Y})_{y,n}\Big]U_{y,n} = \omega\sum_{y,n}\big[\mathbf{X}^\dagger_{x,m}\mathbf{\Delta}\mathbf{X}_{y,n}-\mathbf{Y}^\dagger_{x,m}\mathbf{\Delta}\mathbf{Y}_{y,n}\big]U_{y,n}. \quad (28)$$

The TDA is usually a good approximation to full TDDFT,[40] for both excitation energies and excited-state geometries, and is computationally simpler as this approximation amounts to neglecting the relatively small elements of $\mathbf{Y}$.

Neglecting **B** in Eq. (28) affords the TDA(MI) working equation,

$$\sum_{y,n} \mathbf{X}^{\dagger}_{x,m} \mathbf{A} \mathbf{X}_{y,n} U_{y,n} = \omega \sum_{y,n} \mathbf{X}^{\dagger}_{x,m} \boldsymbol{\Delta} \mathbf{X}_{y,n} U_{y,n}. \quad (29)$$

2. Orthogonality between the occupied space and the virtual space

In the TDDFT working equation with non-orthogonal MOs [Eq. (23)], a new set of virtual orbitals $\widetilde{\phi}_a$ is introduced to guarantee orthogonality between the occupied and virtual spaces. If the conventional ground-state SCF converges with the condition $[\hat{f}_0, \hat{\rho}_0] = 0$, this orthogonality is automatically satisfied and $\widetilde{\phi}_a = \phi_a$, with $\widetilde{\phi}_a$ as defined in Eq. (21).

In Stoll's SCF(MI) method,[31,38] however, $[\hat{f}_0, \hat{\rho}_0] \neq 0$ upon convergence and thus the virtual space for the supersystem is not orthogonal to the occupied space. In the case of this constrained variational SCF method, it is necessary to project the occupied space out of the space spanned by the virtual orbitals, in order to prevent the appearance of low-lying excited states contaminated by the ground state. After projection, Coulomb and exchange couplings between monomers remain in TDDFT(MI), but not orbital overlap interactions.

Through first order in perturbation theory, the electronic coupling for singlet excitation energy transfer consists of three terms: a Coulomb coupling, a Dexter-type exchange coupling, and an overlap (or charge-transfer) coupling,[42] the latter two of which are considered short-range coupling effects. Viewed in this way, only the charge-transfer coupling is omitted in TDDFT(MI).

Above, we introduced a local excitation approximation for TDDFT(MI), and in conjunction with neglect of explicit charge-transfer terms between monomers this amounts to a lack of orbital relaxation that essentially guarantees that excitation energies will be significantly overestimated. To prevent such a deleterious effect on excitation energies, we retain the partial mixing between the occupied space and the virtual space, which preserves the block-diagonal nature of the one-electron part of the matrices **A** and **B** in Eqs. (24) and (25), but partly includes the short-range charge-transfer effect yet without any artificial mixing between ground and excited states.

In contrast to the MOs $\{\widetilde{\phi}_i, \widetilde{\phi}_a\}$ defined in Eqs. (20) and (21), the new, modified MO space $\{\widetilde{\phi}_i, \phi_a\}$ will consist of the transformed occupied orbitals [Eq. (20)] but unchanged ALMO virtual orbitals. In the modified MO representation, the monomer transition densities are expanded as

$$\delta\hat{\rho}_{x,m} = \sum_{a,i\subset x} X_{ai,m} |\phi_a\rangle\langle\widetilde{\phi}_i| + \sum_{a,i\subset x} Y_{ai,m} |\widetilde{\phi}_i\rangle\langle\phi_a|. \quad (30)$$

3. Block locality in energy

The SCF(MI) method involves solving an eigenvalue equation that is block-diagonal based on fragments. For fragment x, this equation is

$$\hat{f}_x |\phi_{xp}\rangle = |\phi_{xp}\rangle \epsilon_{xp}, \quad (31)$$

where

$$\hat{f}_x = (1 - \hat{\rho} + \hat{\rho}^{\dagger}_x) \hat{f} (1 - \hat{\rho} + \hat{\rho}_x) \quad (32)$$

is the projected Fock operator for fragment x. The fragment density operator is

$$\hat{\rho}_x = |\phi^{xi}\rangle\langle\phi_{xi}|, \quad (33)$$

where

$$|\phi^{xi}\rangle = \sum_{yj} S^{-1}_{xi,yj} |\phi_{yj}\rangle. \quad (34)$$

Upon SCF(MI) convergence, the ALMOs are orthogonal within each fragment,

$$\langle\phi_{xp}|\phi_{xq}\rangle = \delta_{pq}. \quad (35)$$

The projected Fock matrix has matrix elements

$$\langle\phi_{xi}|\hat{f}_x|\phi_{xj}\rangle = \langle\widetilde{\phi}_{xi}|\hat{f}|\widetilde{\phi}_{xj}\rangle = \epsilon_{xi}\,\delta_{ij}, \quad (36a)$$

$$\langle\phi_{xa}|\hat{f}_x|\phi_{xb}\rangle = \langle\widetilde{\phi}_{xa}|\hat{f}|\widetilde{\phi}_{xb}\rangle = \epsilon_{xa}\,\delta_{ab}, \quad (36b)$$

$$\langle\phi_{xa}|\hat{f}_x|\phi_{xi}\rangle = \langle\widetilde{\phi}_{xa}|\hat{f}|\widetilde{\phi}_{xi}\rangle = 0. \quad (36c)$$

The Fock operator in new ALMO representation can therefore be expressed as

$$\widetilde{f}_{xp,xq} = \delta_{pq}\,\epsilon_{xp}, \quad (37)$$

meaning that the ground-state Hamiltonian in the new ALMO representation is block diagonal for SCF(MI). Another interesting point is that without the explicit charge-transfer terms, the ground-state SCF convergence condition is satisfied within the monomer-excited state space,

$$\left[\hat{\rho},\ \hat{f}\right] \delta\hat{\rho}_{x,m} = 0. \quad (38)$$

In practice, this prevents the appearance of the sort of low-energy, artificial excited states that were discussed in Section II D 2.

4. Localized method for the occupied orbitals

In order to solve the CIS(MI), TDA(MI), or TDDFT(MI) eigenvalue equation, it is necessary to compute contractions between Fock-like matrices and transition densities in the $\{\widetilde{\phi}_i, \phi_a\}$ representation, which still spreads over the whole system. The bottleneck for excitation energy calculations is the construction of these Fock-like matrices. This can be dramatically simplified by exploiting a local approximation for the new occupied MOs in each fragment.[43]

Following Ref. 43, we define a projected molecular orbital $\widetilde{\phi}'_i$ that is expanded within a local subset of AOs for each $\widetilde{\phi}_i$, and then replace each new occupied MO with the corresponding projected MO for the purpose of computing the Fock-like matrices. Expanding the projected MOs in monomer subsets of atomic orbitals χ_μ,

$$\widetilde{\phi}'_i = \sum_{\mu,i\subset x} C'_{\mu i}\,\chi_\mu, \quad (39)$$

the expansion coefficients can be computed by minimizing the functional

$$d = \int \left[\widetilde{\phi}'_i(\mathbf{r}) - \widetilde{\phi}_i(\mathbf{r})\right]^2 d\mathbf{r}. \quad (40)$$

This minimization amounts to the solution of linear equations

$$\sum_{\nu, i\subset x} S_{\mu\nu} C'_{\nu,i} = \langle \widetilde{\phi}_i | \chi_\mu \rangle. \tag{41}$$

The orbitals $\widetilde{\phi}'_i$ are usually very good approximations to the original $\widetilde{\phi}_i$, but in the former representation, it is only necessary to build Fock-like matrices using single-monomer subsets of the supersystem AO basis. To compute the couplings, only dimer subsets of the supersystem AO basis are required.

III. NUMERICAL RESULTS

We have implemented the CIS(MI), TDA(MI), and TDDFT(MI) methods in a locally modified version of Q-Chem.[44] Stoll's SCF(MI) method,[38] as implemented in Q-Chem by Khaliullin *et al.*,[31] is used to compute the ground state ALMOs, which are then used in the subsequent monomer calculations and CIS(MI), TDA(MI), and TDDFT(MI) calculations. We employ two excited states per monomer in the MI calculations [$N_{\text{roots}} = 2$ in Eq. (27)]. To ensure that these roots are well-converged in the ALMO basis, we request ten excited states in each monomer calculation, retaining only the lowest two for the subsequent MI calculations. (Occasionally, small energy differences in the low-lying monomer excitation energies are observed when only two states are requested, as this reduces the number of subspace vectors that are used in the Davidson iterations.) Cartesian coordinates for all of the molecular complexes examined here are available in the supplementary material.[45]

Rather than looking exhaustively at various density functionals, this work is focused on comparing differences between the fragment method and the supersystem method; thus, excitation energies will be computed at the Hartree-Fock level except where otherwise specified. Error in a CIS(MI) calculation, for example, will be defined relative to the corresponding traditional CIS calculation performed on the supersystem. There are several reasons for this choice. First, TDDFT calculations of non-covalent clusters are often beset by spurious charge-transfer excitations,[46] making the TDDFT supersystem benchmarks problematic. Second, it is well known that the virtual orbitals in Kohn-Sham theory tend to be more compact than the corresponding Hartree-Fock virtual orbitals,[47–49] with the former resembling bound-state excitations rather than electron-attached states. For this reason, we expect that the localized approximations introduced here will fare no worse for TDDFT than for CIS. Comparison of CIS(MI) to supersystem CIS results will therefore demonstrate the robustness of the approximations introduced by the MI approach, which is then readily extended to TDDFT(MI) without concern about spurious charge-transfer states.

A. Dimers

We first examine ethylene dimer and naphthalene dimer, parallel-displaced at various intermolecular distances. Monomer geometries were optimized at the B3LYP/6-31G* level and excitation energies were computed at the CIS/6-311G* level.

The first excited state (S_1) is a bit different in these two cases. The S_1 state of ethylene *monomer* has a larger oscillator strength ($f = 0.61$), as compared to that of naphthalene monomer ($f = 0.08$). This implies a more significant Coulomb coupling between the ethylene molecules. Excitation energies for both dimers were calculated for intermolecular distances ranging from 4 to 10 Å, and the interaction energy was found to vary significantly over this range, for both dimers.

Figure 1 shows excitation energies and energy splittings for the two aforementioned dimers, computed at the levels of full (i.e., supersystem) CIS, CIS(MI), and an "uncoupled CIS(MI)" [uCIS(MI)] approach. The latter means a CIS calculation using an isolated monomer ALMO basis, which we do not expect to be an accurate approximation but is interesting for comparative purposes. It can be seen that the S_1 excitation energy computed at the uCIS(MI) level is very close to the monomer excitation energy (which is 8.343 eV for ethylene and 5.142 eV for naphthalene), with a slight deviation because the ALMOs and orbital energies used in the uCIS(MI) calculations for one monomer are affected by the other monomer. As the distance increases, the interaction between the two monomers becomes smaller and the difference decreases. When the distance is large enough, the coupling is very weak and the excitation energies of the dimer can be approximated as[42]

$$\omega_\pm = \omega_{\text{monomer}} \pm V, \tag{42}$$

where the coupling V is equal to half of the energy gap between a pair of coupled, identical monomers,

$$|V| = \tfrac{1}{2}|E_2 - E_1|. \tag{43}$$

The results in Figure 1 agree very well with this energy-gap approach, in that the uCIS(MI) excitation energy curve lies nearly in the middle of two coupled excited states, especially as the distance between the two monomers becomes large.

The supersystem calculation, on the other hand, still exhibits a noticeable energy gap between the upper excited state (S_u) and the lower excited state (S_l), even at a distance of 10 Å. This indicates a significant coupling between the two monomer excitations, which the uCIS(MI) approach, by construction, fails to describe. The CIS(MI) method, however, reproduces the supersystem results very well from 5 to 10 Å, wherein the splitting decreases from 0.246 to 0.025 eV for ethylene and from 0.054 to 0.006 eV for naphthalene.

At 4 Å separation and below, the situation is different. Although there is still qualitative agreement between the CIS(MI) approach and the supermolecular results, the S_u/S_l splitting in the CIS(MI) calculation is much smaller that in the supersystem CIS calculation, e.g., 0.466 eV versus 0.682 eV for ethylene dimer. This is due to the overlap between the two monomer densities at short distance, which cannot be accurately described by the CIS(MI) approach because the local excitation approximation and ALMOs used in CIS(MI) do not properly describe short-range intermolecular interactions. The situation deteriorates if the short-range coupling makes a larger contribution to the total coupling. For the bright state S_u, the long-range Coulomb coupling is still the main contribution to the total coupling while for dark state S_l it is much smaller, which explains the larger error (0.204 eV) for S_l as compared

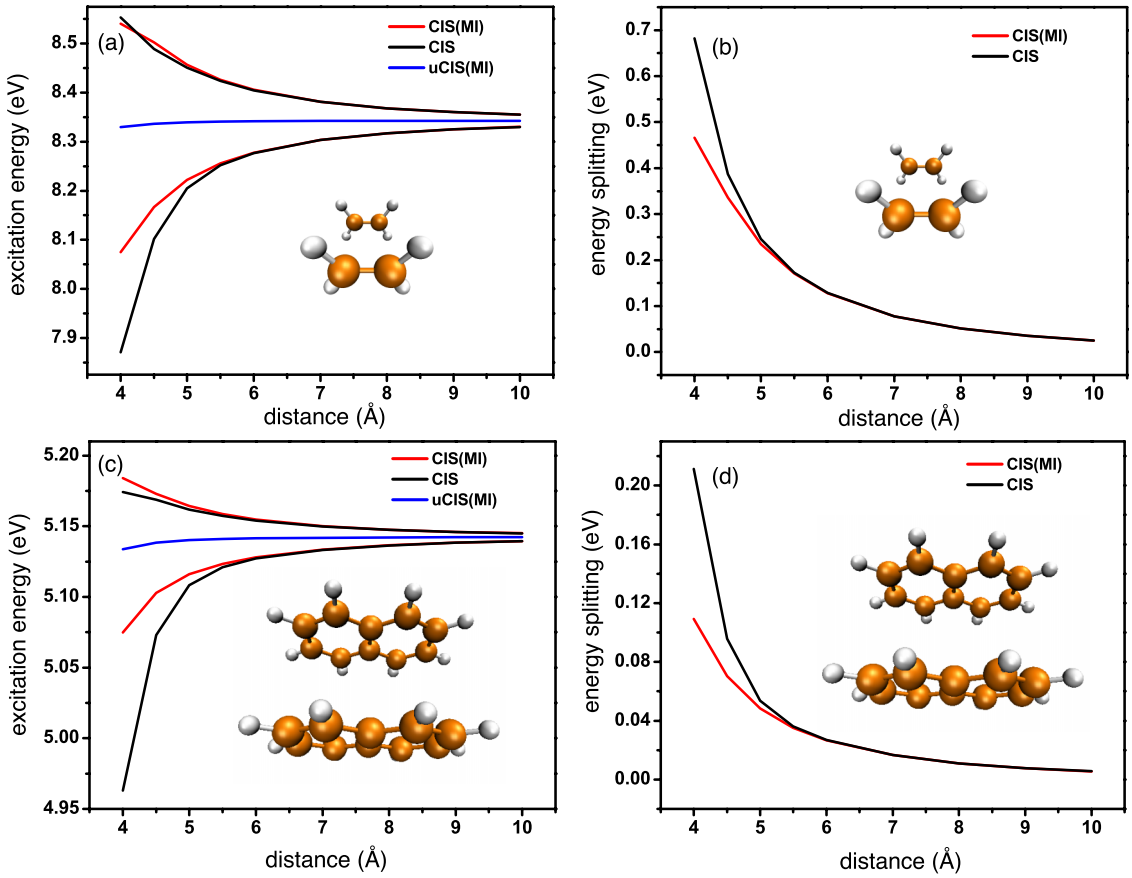

FIG. 1. Excitation energies (on the left) and energy splittings (on the right) from full CIS, CIS(MI), and uCIS(MI) calculations, for ethylene [in (a) and (b)] and naphthalene [in (c) and (d)].

to the smaller error (−0.013 eV) in the case of S_u, for $(C_2H_4)_2$ at 4 Å separation.

For naphthalene dimer, the relative error in the S_u/S_l splitting is larger than that in ethylene dimer because the Coulomb coupling between the excitations on the two monomers is much smaller. At 5 Å separation, the relative error in the splitting is 9.9% for naphthalene but only 4.4% for ethylene. Even for naphthalene dimer, however, the excitation energy of the bright state S_u (5.184 eV) is still quite close to the full CIS result (5.182 eV).

B. Water chains

One-dimensional water chains are chosen as the second test systems, because they have been studied previously using an alternative exciton model.[30] Although somewhat contrived, these systems represent challenging test cases because the distance between monomers is small and short-range effects should be significant. However, some short-range effects are included by virtue of the mixing (non-orthogonality) of the occupied orbitals and the virtual orbitals, and it is necessary to assess the performance of CIS(MI) on a range of systems. Fig. 2 shows the structure of a one-dimensional water chain. The geometrical configuration of these water chains is a little different from that in Ref. 30; here, the O–H bond length is set to 0.96 Å and the H–O–H angle is set to 104.45°. The hydrogen bond length between neighboring water molecules is taken to be either 1.5, 2.2, or 3.0 Å.

Table I lists the excitation energy errors for CIS(MI), as compared to full supersystem CIS results, for water chains with 8 and 16 monomers, using several different basis sets. Results for the two systems are similar and errors in the lowest excitation energy are mostly on the order of 0.1 eV. Errors obtained in the 6-31G and 6-31G* basis sets are similar, suggesting that polarization functions do not affect the performance of the CIS(MI) approximation, even at short separations. However, errors are somewhat larger when the basis set is 6-31+G*, up to almost 0.3 eV at 1.5 Å separation.

The relatively large errors in $S_0 \rightarrow S_2$ excitation energies in the 6-31+G* basis set have two origins: short-range coupling between the monomers and coupling to the S_1 state. The latter effect causes errors in the S_1 excitation energy to be magnified in S_2. As discussed in Ref. 30, the $S_0 \rightarrow S_1$ excitation at 1.5 Å separation mainly involves the HOMO but involves

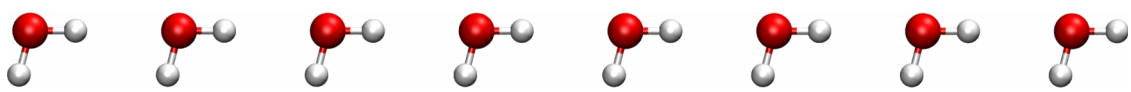

FIG. 2. A one-dimensional water chain.

TABLE I. Difference in calculated $S_0 \rightarrow S_1$ and $S_0 \rightarrow S_2$ excitation energies in water chain systems, comparing the CIS(MI) and supersystem CIS methods.

		Excitation energy error/eV					
		6-31G		6-31G*		6-31+G*	
	R/Å	S_1	S_2	S_1	S_2	S_1	S_2
$(H_2O)_8$	1.5	0.10	0.11	0.08	0.10	0.12	0.25
	2.2	0.06	0.06	0.06	0.07	0.10	0.15
	3.0	0.08	0.08	0.09	0.09	0.14	0.14
$(H_2O)_{16}$	1.5	0.10	0.14	0.07	0.13	0.11	0.29
	2.2	0.07	0.06	0.06	0.07	0.10	0.16
	3.0	0.08	0.08	0.10	0.10	0.14	0.15

a variety of virtual orbitals. This means that there is a lot of charge-transfer-type excitation mixed into the S_1 state at short separation, excitations that are absent in CIS(MI). These charge-transfer effects become more important in the presence of diffuse basis functions. The $S_0 \rightarrow S_2$ excitation originates from many MOs and thus several water molecules make significant contributions. In an excitonic picture, then, the coupling of monomer excited states in S_1 is much weaker as compared to S_2, which couples excited states on many different water monomers. Only monomer-excited basis states are considered in CIS(MI) so it is more difficult to describe these multi-region excitations. Nevertheless, given that CIS(MI) can be extended to very large clusters, errors in CIS(MI) excitation energies remain acceptably small.

C. Water clusters

We next investigate 8 low-energy conformations of the $(H_2O)_6$ cluster and 12 low-energy conformations of $(H_2O)_{20}$. (Cluster geometries were taken from Refs. 50 and 51.) The lowest-lying excitation in one such cluster is depicted in Fig. 3, and clearly involves the $1b_1 \rightarrow 4a_1$ transition on two different water molecules. This example demonstrates that excited states in water clusters need not be confined to a single water molecule but can exhibit non-trivial excitonic coupling between multiple monomers.

CIS(MI) excitation energy errors for the first and second excited states are shown in Fig. 4 for three different basis sets. As above, 6-31G and 6-31G* yield very similar errors, and these errors are <0.05 eV relative to supersystem CIS results, but the performance for 6-31+G* is quite different. In the latter case, errors range from 0.04 to 0.18 eV for $(H_2O)_6$. Errors for $(H_2O)_{20}$ are slightly larger, but again the 6-31G and 6-31G* basis sets afford good agreement between CIS and CIS(MI) results, with differences <0.1 eV in most cases, while for 6-31+G* the maximum difference is 0.23 eV.

Considering results for these clusters and for water chains, we can say that overall for water, the CIS(MI) method affords a nearly quantitative description in the absence of diffuse functions. Semi-quantitative results are obtained, even in the presence of diffuse functions, with differences of 0.2–0.3 eV relative to full CIS.

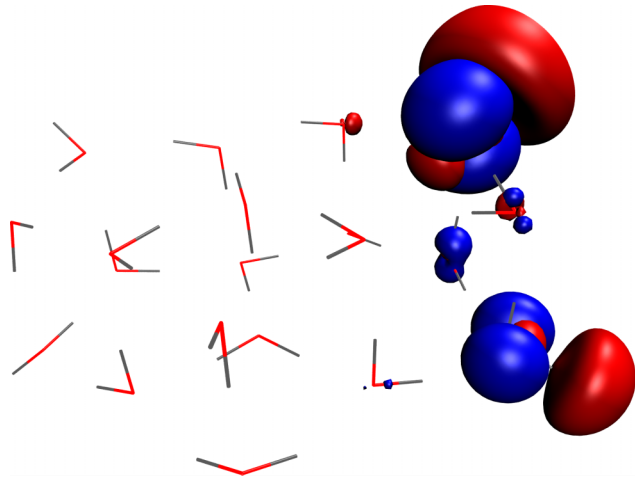

FIG. 3. An excitation of $(H_2O)_{20}$ computed at the CIS/6-31G* level and plotted with an isocontour of 0.002 a.u. Attachment and detachment densities[52] are shown in red and blue, respectively, and indicate that this particular excitation is characterized by excitonic coupling, primarily between two water molecules.

D. Solvated chromophores

Next, we consider an acetone molecule in $(H_2O)_n$ and a benzene molecule in $(H_2O)_n$, as model systems for a polar and a non-polar solute dissolved in water. Ten snapshots for each system were extracted from room temperature, solution-phase molecular dynamics simulation, using cut-off radii of 3, 4, and 5 Å from the solute. Tables II and III list the errors in the CIS(MI) excitation energies for the $S_0 \rightarrow S_1$ excitation.

CIS(MI) results are quite accurate for both systems, with average deviations of ~0.02 eV in acetone–water and ~0.07 eV in benzene–water, even for the 6-31+G* basis set. The basis set effect is very small in this case because the excitation is mainly localized on the solute molecule, i.e., excitonic delocalization is negligible. The cluster size dependence of the errors is also quite small, meaning that CIS(MI) can potentially be used to include a large number of explicit solvent molecules into an excited-state calculation, without much loss of accuracy provided that the excitation is mostly localized on the chromophore.

E. Naphthalene diimide-lysine (NDI) aggregates

Molecular self-assembly can generate complex nanoscale structures with desirable properties, based on non-covalently packed chromophore units. Recently, an organic semiconductor nanotube formed from NDI subunits has been reported,[53,54] which appears to exhibit rapid excited-state exciton migration, and an atomic-resolution structural model has also been reported.[24] Here, we will test the CIS(MI) method on $(NDI)_n$ sub-structures (n = 2, 4, 6, and 9) that are extracted from the nanotube structural model. In these substructures, the lysine side chains have been replaced by methyl groups as described in Ref. 24.

Figure 5 shows the structure of $(NDI)_9$, and the smaller $(NDI)_n$ structures were cut out of this one. Excitation energies for several $(NDI)_n$ clusters extracted from the nanotube structure are listed in Table IV. Results for three different

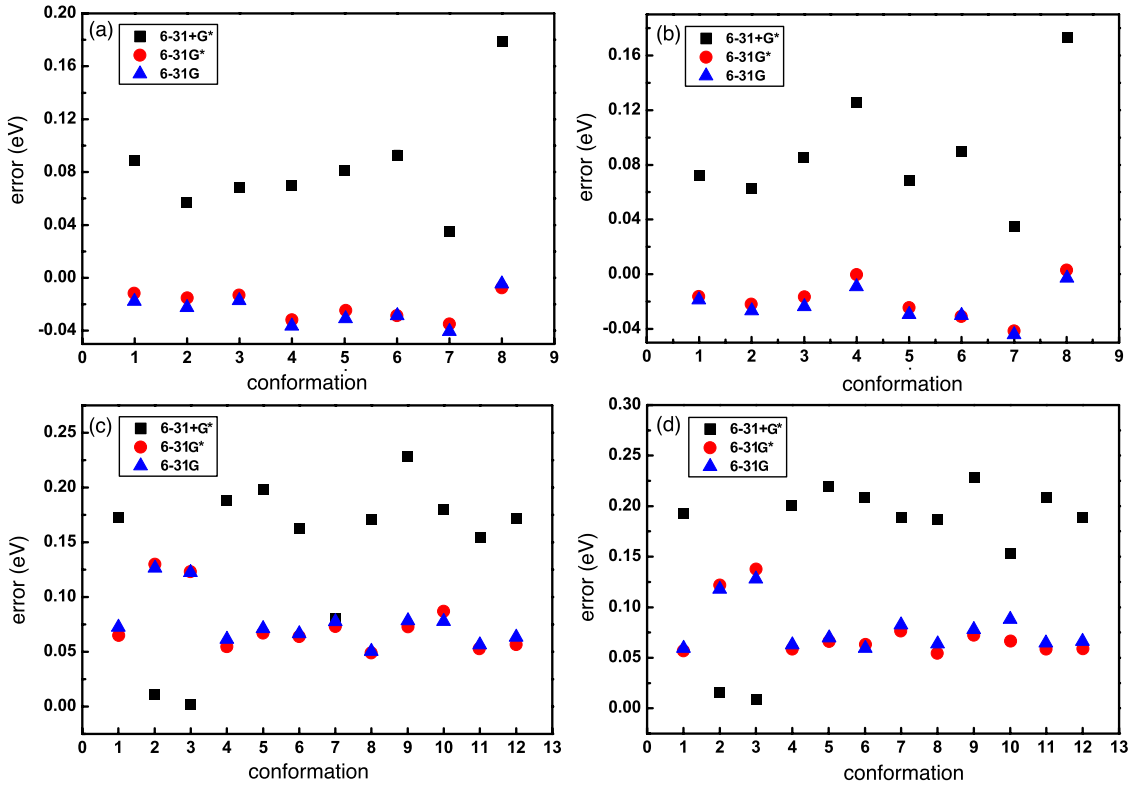

FIG. 4. CIS(MI) excitation energy errors for (a) the S_1 state of $(H_2O)_6$, (b) the S_2 state of $(H_2O)_6$, (c) the S_1 state of $(H_2O)_{20}$, and (d) the S_2 state of $(H_2O)_{20}$.

dimers are shown; these correspond to the three different nearest-neighbor directions in the nanotube, along which energy migration might be expected to occur. We call these the "ring," "tube," and "diagonal" directions, as defined in Fig. 3(a) of Ref. 24. In Table IV, we list excitation energies for both the bright states S_u of the three dimers as well as the state that is strongly coupled to it. Recognizing that the coupling matrix element between these two states should be approximately half of the energy splitting between S_u and S_l, we estimate couplings of ≈0.08 eV (tube direction), ≈0.04 eV (ring direction), and ≈0.02 eV (diagonal direction). These values are consistent with the couplings reported in Ref. 24 based on full TDDFT calculations.

Table IV also lists TDA(MI) excitation energies for aggregates of $(NDI)_4$, $(NDI)_6$, and $(NDI)_9$, along with supersystem TDA results. The errors for the singlet excitations are much larger than in the solvated chromophores of Section III D, yet they remain acceptably small. In the former systems, the first singlet excited state of solute is weakly coupled to the solvent molecules, but in these NDI aggregates, the coupling along the tube direction is strong. This manifests as differences of up to 0.1 eV between TDA(MI) and TDA excitation energies for the "tube" structure of $(NDI)_2$. In the larger NDI aggregates, TDA(MI) errors in the S_1 and T_1 excitation energies are <0.1 eV, but the error in the bright state is somewhat larger (∼0.2 eV). This error originates in the missing short-range

TABLE II. Difference in calculated S_1 excitation energies (in eV) in hydrated acetone, comparing CIS(MI) to CIS for clusters of increasing radius.

	$R = 3.0$ Å			$R = 4.0$ Å			$R = 5.0$ Å		
Configuration	6-31G	6-31G*	6-31+G*	6-31G	6-31G*	6-31+G*	6-31G	6-31G*	6-31+G*
1	−0.008	−0.008	0.009	−0.009	−0.009	0.006	−0.014	−0.014	0.006
2	−0.012	−0.011	0.031	−0.013	−0.012	0.034	−0.015	−0.015	0.033
3	−0.024	−0.026	0.013	−0.027	−0.029	0.013	−0.029	−0.031	0.013
4	−0.021	−0.026	0.027	−0.034	−0.038	0.020	−0.041	−0.045	0.018
5	−0.005	−0.007	0.023	−0.019	−0.020	0.016	−0.017	−0.019	0.022
6	−0.033	−0.034	0.004	−0.047	−0.047	0.003	−0.042	−0.043	0.005
7	−0.005	−0.005	0.010	−0.012	−0.012	0.016	−0.010	−0.010	0.017
8	0.004	0.005	0.006	0.005	0.006	0.010	0.006	0.007	0.011
9	−0.008	−0.010	0.016	−0.021	−0.021	0.010	−0.024	−0.025	0.009
10	0.014	0.012	0.025	−0.021	−0.020	0.010	−0.020	−0.020	0.010
MAE	0.013	0.014	0.016	0.021	0.022	0.014	0.022	0.023	0.015

TABLE III. Difference in calculated S_1 excitation energies (in eV) in hydrated benzene, comparing CIS(MI) to CIS for clusters of increasing radius.

	$R = 3.0$ Å			$R = 4.0$ Å			$R = 5.0$ Å		
Configuration	6-31G	6-31G*	6-31+G*	6-31G	6-31G*	6-31+G*	6-31G	6-31G*	6-31+G*
1	0.046	0.045	0.044	0.056	0.055	0.049	0.058	0.057	0.065
2	0.087	0.080	0.070	0.104	0.095	0.090	0.110	0.099	0.098
3	0.084	0.078	0.073	0.075	0.073	0.066	0.073	0.071	0.062
4	0.095	0.092	0.089	0.098	0.096	0.088	0.103	0.099	0.112
5	0.052	0.052	0.049	0.064	0.063	0.061	0.065	0.064	0.072
6	0.048	0.046	0.034	0.065	0.062	0.043	0.060	0.059	0.049
7	0.037	0.037	0.036	0.045	0.045	0.045	0.045	0.045	0.045
8	0.068	0.066	0.058	0.076	0.075	0.071	0.078	0.076	0.073
9	0.047	0.045	0.048	0.065	0.062	0.062	0.068	0.065	0.066
10	0.056	0.055	0.053	0.056	0.056	0.044	0.055	0.055	0.050
MAE	0.062	0.060	0.055	0.071	0.060	0.062	0.071	0.069	0.069

interactions and delocalization of the excited state, especially for the tube direction, but the very small magnitude of the errors suggests that the TDA(MI) methodology is able to account for these effects well enough.

Since Sec. III F focuses on the efficiency of the TDDFT(MI) method, we note here that it takes ~80 h to solve the supersystem TDA equations for $(NDI)_9$ but only about 2 h to solve the TDA(MI) equations for the same system, on a single processor.

F. Efficiency

A calculation at the TDDFT(MI), TDA(MI), or CIS(MI) level involves the following steps: (1) a ground-state calculation for the supersystem at the SCF(MI) level; (2) isolated excited state calculations for each subsystem; (3) assembling the one-electron part of the supersystem Fock matrix and the couplings amongst the monomer-excited basis states; and (4) the iterative diagonalization process. The most time-consuming steps are the ground-state calculation and the coupling calculations. In the ground-state SCF(MI) calculation, the diagonalization step has been significantly improved.[31]

The computational time for the couplings depends linearly on the number of them that is required, which is M^2 for a subspace of dimension M assembled from the monomer excited states. Typically, $M = N_{\text{fragment}} \times N_{\text{roots}}$. The time needed to compute each coupling grows as $O(N^x_{\text{sub-AO}})$ where $2 \le x \le 4$ (reflecting SCF-like cost), and $N_{\text{sub-AO}}$ is the number of basis function in a subsystem (dimer) AO basis set.

Traditional supersystem CIS, TDA, or TDDFT calculations employ Davidson iteration to diagonalize the

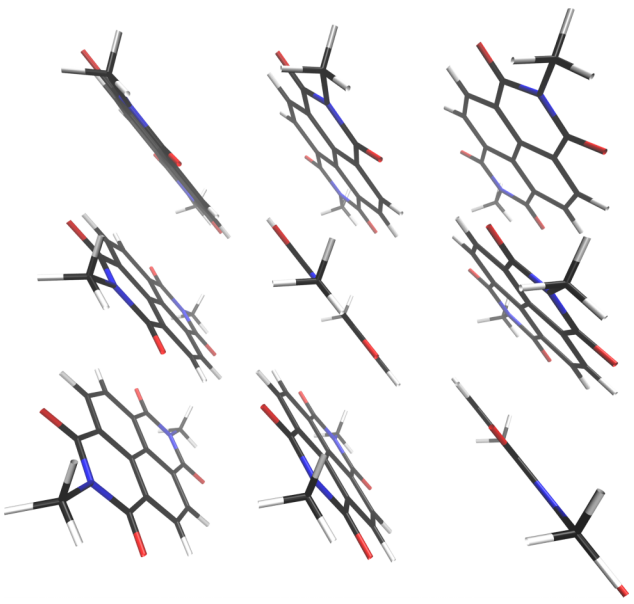

FIG. 5. Structure of $(NDI)_9$.

TABLE IV. Excitation energies (in eV) of clusters of methylated NDI, comparing TDA(MI) and TDA results at the Hartree-Fock level and also using the LRC-ωPBE functional.[55] For the dimers, the states are labeled S_u (upper state) and S_l (lower state). For the larger aggregates, S_b is the lowest bright state.

Structure	Method	State	TDA(MI)	TDA
$(NDI)_2$ ring	HF/6-31G*	S_l	4.073	4.066
		S_u	4.191	4.184
	DFT/6-31G*	S_l	3.799	3.791
		S_u	3.924	3.916
$(NDI)_2$ tube	HF/6-31G*	S_l	4.054	4.022
		S_u	4.213	4.135
	DFT/6-31G*	S_l	3.774	3.731
		S_u	3.949	3.825
$(NDI)_2$ diagonal	HF/6-31G*	S_l	4.086	4.071
		S_u	4.169	4.155
	DFT/6-31G*	S_l	3.819	3.804
		S_u	3.904	3.891
$(NDI)_4$	HF/6-31G	T_1	1.796	1.778
		S_1	4.091	4.047
		S_b	4.393	4.270
$(NDI)_6$	HF/6-31G	T_1	1.796	1.755
		S_1	4.076	3.990
		S_b	4.469	4.267
$(NDI)_9$	HF/6-31G	T_1	1.785	1.737
		S_1	4.070	3.970
		S_b	4.537	4.300

TABLE V. Ratio of the total CIS time to the total CIS(MI) time for the acetone–water systems from Table II.

Configuration	6-31G	6-31G*	6-31+G*
1	9	12	18
2	7	8	13
3	8	13	15
4	8	9	11
5	7	11	13
6	9	10	10
7	9	12	13
8	8	11	12
9	10	14	16
10	6	8	10
Average	8	11	13

singly-excited block of the configuration-interaction Hamiltonian. The number of iterations required to reach convergence varies with the system as well as the number of desired eigenvalues, but is typically 10–30 iterations when several (but $\ll$30) eigenvalues are requested. In each iteration, the Fock-like matrix contraction (digestion step) scales as $O(N^x_{\text{super-AO}})$ where $N_{\text{super-AO}}$ is the size of the total basis set. The number of digestions that is required at each iteration is equal to the number of unconverged excited states.

Table V lists the ratio of the total time required for CIS and CIS(MI) calculations of the acetone–water system (5 Å cutoff) that was discussed in Section III D. All calculations were performed on a single processor. The speed-up ratio is a factor of 8, even for the small 6-31G basis set, and increases as the basis set is enlarged, reaching a factor of 13 for 6-31+G*. Most of the CIS(MI) time is spent in the ground-state SCF(MI) calculation. In acetone–water configuration #1, for example, the SCF(MI) step takes 633 s while the entire calculation takes only 790 s, on a single processor.

IV. SUMMARY AND CONCLUSIONS

A non-orthogonal formulation of time-dependent density functional theory in the frequency domain has been derived based on the absolutely-localized MO representation.[31–33] An efficient implementation for collections of weakly interacting molecules is then obtained by applying several approximations: (1) a local (monomer) excitation approximation; (2) an efficient localization method; and (3) a single-step Davidson algorithm for solving the working equations. The computational effort to solve these CIS(MI), TDA(MI), and TDDFT(MI) working equations scales as $O(N^2_{\text{fragment}}N^2_{\text{roots}}N^x_{\text{sub-AO}})$ where $N_{\text{sub-AO}}$ is the number of AOs on a dimer subsystem, and the exponent x (with $2 \le x \le 4$) reflects the cost of forming Fock-like matrices and depends on the details of the system and the efficiency of the electron repulsion integral code.

Numerical examples presented herein demonstrate that these new "MI" methods reliably reproduce excitation energies from supermolecular CIS, TDA, and TDDFT calculations in various non-covalent systems. This is especially true for systems composed of explicit solvent molecules surrounding a chromophore. At the same time, calculations in aggregates of naphthalene diimide, a monomer that forms the structural building block of self-assembling organic nanotubes,[24,53,54] demonstrate that the excited-state MI methods are also applicable to systems composed of multiple, electronically coupled chromophores.

The present work complements other recently developed *ab initio* exciton models.[20,30] These include the "renormalized exciton method" of Ref. 30, whose cost scales like that of an excited-state calculation on a dimer of fragments. In the present approach, however, only couplings between dimers (and not entire excited-state dimer calculations) are required, so that the prefactor for our approach should be smaller even if the formal computational scaling with system size is about the same. An *ab initio* Frenkel-Davydov model developed previously in our group[20] only requires excited-state calculations on monomers; however, evaluating the couplings between these monomer excitations requires a contraction involving the entire supersystem, which is a significant expense in large systems. (A low-cost version that restricts this contraction to regions that are localized in space is currently under development in our group.[56]) In all of these models, parallelization over monomers and/or dimers is necessary for efficiency, but is straightforward.

At short intermolecular separations, problems can arise due to a breakdown of the local excitation approximation in the monomer excited-state basis. In such situations, short-range effects play a more important role and are only partially included via overlap between the occupied space and the virtual space. In order to more accurately describe short-range effects, the explicit inclusion of charge-transfer terms would be necessary. Nevertheless, errors engendered at short range are found to be no worse than 0.2–0.3 eV for the systems considered here, and no worse than ~0.1 eV for the naphthalene diimide aggregates. This is not significantly worse than the $\lesssim$0.1 eV errors engendered by existing *ab initio*-type exciton models.[20,30]

The most appealing aspect of the TDDFT(MI) method is its computational efficiency. The $O(N^2_{\text{fragment}})$ scaling means that the computational time increases only quadratically with system size, and the pre-factor is small. Furthermore, the use of locality in both energy and space leads to very small couplings in weakly interacting systems, which means that only a few couplings are non-negligible. In weakly coupled systems, such as solvated chromophores, only the diagonal elements of the **A** and **B** matrices are necessary to extract the lowest excitation energy. Finally, it is worth mentioning that this method is naturally suited to a massively parallel implementation because the coupling calculations are completely independent of one another.

ACKNOWLEDGMENTS

As we were finalizing this manuscript for submission, we became aware of an alternative ALMO-based CIS algorithm in preparation by Closser *et al.*,[34] to which we wish to draw the reader's attention. We thank Martin Head-Gordon for providing a preprint of Ref. 34.

This work was supported by the U.S. Department of Energy, Office of Basic Energy Sciences, Division of Chemical Sciences, Geosciences, and Biosciences under Award No.

DE-SC0008550, and by the National Science Foundation under Grant No. CHE-1300603. Calculations were performed at the Ohio Supercomputer Center[57] under Project No. PAA-0003. J.M.H. is a Camille Dreyfus Teacher-Scholar.

[1]M. E. Casida, "Time-dependent density functional response theory for molecules," in *Recent Advances in Density Functional Methods, Part I*, Recent Advances in Computational Chemistry Vol. I, edited by D. P. Chong (World Scientific, River Edge, NJ, 1995), Chap. 5, pp. 155–192.
[2]M. Petersilka, U. J. Grossmann, and E. K. U. Gross, Phys. Rev. Lett. **76**, 1212 (1996).
[3]N. T. Maitra, K. Burke, H. Appel, E. K. U. Gross, and R. van Leeuwen, "Ten topical questions in time-dependent density functional theory," in *Reviews of Modern Quantum Chemistry*, edited by K. D. Sen (World Scientific, 2002), Vol. 1, pp. 1186–1225.
[4]M. A. L. Marques and E. K. U. Gross, Annu. Rev. Phys. Chem. **55**, 427 (2004).
[5]S. J. A. van Gisbergen, J. G. Snijders, and E. J. Baerends, Comput. Phys. Commun. **118**, 119 (1999).
[6]A. Dreuw and M. Head-Gordon, Chem. Rev. **105**, 4009 (2005).
[7]M. E. Casida, J. Mol. Struct.: THEOCHEM **914**, 3 (2009).
[8]J. Liu and W. Liang, J. Chem. Phys. **135**, 184111 (2011).
[9]S. J. A. van Gisbergen, C. F. Guerra, and E. J. Baerends, J. Comput. Chem. **21**, 1511 (2000).
[10]C. Y. Yam, Q. Zhang, F. Wang, and G. H. Chen, Chem. Soc. Rev. **41**, 3821 (2012).
[11]S. Coriani, S. Høst, B. Jansìk, L. Thøgersen, J. Olsen, P. Jørgensen, S. Reine, F. Pawłowski, T. Helgaker, and P. Sałek, J. Chem. Phys. **126**, 154108 (2007).
[12]T. Kjærgaard, P. Jøgensen, J. Olsen, S. Coriani, and T. Helgaker, J. Chem. Phys. **129**, 054106 (2008).
[13]M. E. Casida and T. A. Wesołowski, Int. J. Quantum Chem. **96**, 577 (2004).
[14]J. Neugebauer, M. J. Louwerse, E. J. Baerends, and T. A. Wesołowski, J. Chem. Phys. **122**, 094115 (2005).
[15]J. Neugebauer, J. Chem. Phys. **126**, 134116 (2007).
[16]C. Yam, S. Yokojima, and G. Chen, Phys. Rev. B **68**, 153105 (2003).
[17]G. Cui, W. Fang, and W. Yang, Phys. Chem. Chem. Phys. **12**, 416 (2009).
[18]F. Wu, W. Liu, Y. Zhang, and Z. Li, J. Chem. Theory Comput. **7**, 3643 (2011).
[19]D. Abramavicius, B. Palmieri, D. V. Voronine, F. Šanda, and S. Mukamel, Chem. Rev. **109**, 2350 (2009).
[20]A. F. Morrison, Z.-Q. You, and J. M. Herbert, J. Chem. Theory Comput. **10**, 5366 (2014).
[21]G.-J. Zhao and K.-L. Han, J. Phys. Chem. A **111**, 9218 (2007).
[22]J. Liu and W. Liang, J. Chem. Phys. **138**, 024101 (2013).
[23]A. W. Lange and J. M. Herbert, J. Am. Chem. Soc. **131**, 3913 (2009).
[24]M. Gao, S. Paul, C. D. Schwieters, Z.-Q. You, H. Shao, J. M. Herbert, J. R. Parquette, and C. P. Jaroniec, J. Phys. Chem. C **119**, 13948 (2015).
[25]J. Frenkel, Phys. Rev. **37**, 17 (1931).
[26]A. S. Davydov, Sov. Phys. - Usp. **530**, 145 (1964).
[27]K. Ohta, M. Yang, and G. R. Fleming, J. Chem. Phys. **115**, 7609 (2001).
[28]F. Pan, F. Gao, W. Liang, and Y. Zhao, J. Phys. Chem. B **113**, 14581 (2009).
[29]A. Sisto, D. R. Glowacki, and T. J. Martinez, Acc. Chem. Res. **47**, 2857 (2014).
[30]Y. Ma and H. Ma, J. Phys. Chem. A **117**, 3655 (2013).
[31]R. Z. Khaliullin, M. Head-Gordon, and A. T. Bell, J. Chem. Phys. **124**, 204105 (2006).
[32]R. Z. Khaliullin, E. A. Cobar, R. C. Lochan, A. T. Bell, and M. Head-Gordon, J. Phys. Chem. A **111**, 8753 (2007).
[33]L. D. Jacobson and J. M. Herbert, J. Chem. Phys. **134**, 094118 (2011).
[34]K. D. Closser, Y. Shao, Q. Ge, and M. Head-Gordon, "A local excited state method using single substitutions in the absolutely localized molecular orbital basis with application to spectra of large helium clusters" (unpublished).
[35]C. R. Jacob, J. Neugebauer, L. Jensen, and L. Visscher, Phys. Chem. Chem. Phys. **8**, 2349 (2006).
[36]E. R. Davidson, J. Comput. Phys. **17**, 87 (1975).
[37]R. E. Stratmann, G. E. Scuseria, and M. J. Frisch, J. Chem. Phys. **109**, 8218 (1998).
[38]H. Stoll, G. Wagenblast, and H. Preuss, Theor. Chem. Acc. **57**, 169 (1980).
[39]T. Nagata, O. Takahashi, K. Saito, and S. Iwata, J. Chem. Phys. **115**, 3553 (2001).
[40]S. Hirata and M. Head-Gordon, Chem. Phys. Lett. **314**, 291 (1999).
[41]M. A. L. Marques and A. Rubio, "Time versus frequency space techniques," in *Time-Dependent Density Functional Theory*, Lecture Notes in Physics Vol. 706, edited by M. A. L. Marques *et al.* (Springer, Berlin, 2006), Chap. 15, pp. 227–243.
[42]Z.-Q. You and C.-P. Hsu, Int. J. Quantum Chem. **114**, 102 (2014).
[43]C. Zhang, D. Yuan, Y. Guo, and S. Li, J. Chem. Theory Comput. **10**, 5308 (2014).
[44]Y. Shao, Z. Gan, E. Epifanovsky, A. T. B. Gilbert, M. Wormit, J. Kussmann, A. W. Lange, A. Behn, J. Deng, X. Feng, D. Ghosh, M. Goldey, P. R. Horn, L. D. Jacobson, I. Kaliman, R. Z. Khaliullin, T. Kús, A. Landau, J. Liu, E. I. Proynov, Y. M. Rhee, R. M. Richard, M. A. Rohrdanz, R. P. Steele, E. J. Sundstrom, H. L. Woodcock III, P. M. Zimmerman, D. Zuev, B. Albrecht, E. Alguire, B. Austin, G. J. O. Beran, Y. A. Bernard, E. Berquist, K. Brandhorst, K. B. Bravaya, S. T. Brown, D. Casanova, C.-M. Chang, Y. Chen, S. H. Chien, K. D. Closser, D. L. Crittenden, M. Diedenhofen, R. A. DiStasio, Jr., H. Dop, A. D. Dutoi, R. G. Edgar, S. Fatehi, L. Fusti-Molnar, A. Ghysels, A. Golubeva-Zadorozhnaya, J. Gomes, M. W. D. Hanson-Heine, P. H. P. Harbach, A. W. Hauser, E. G. Hohenstein, Z. C. Holden, T.-C. Jagau, H. Ji, B. Kaduk, K. Khistyaev, J. Kim, J. Kim, R. A. King, P. Klunzinger, D. Kosenkov, T. Kowalczyk, C. M. Krauter, K. U. Lao, A. Laurent, K. V. Lawler, S. V. Levchenko, C. Y. Lin, F. Liu, E. Livshits, R. C. Lochan, A. Luenser, P. Manohar, S. F. Manzer, S.-P. Mao, N. Mardirossian, A. V. Marenich, S. A. Maurer, N. J. Mayhall, C. M. Oana, R. Olivares-Amaya, D. P. O'Neill, J. A. Parkhill, T. M. Perrine, R. Peverati, P. A. Pieniazek, A. Prociuk, D. R. Rehn, E. Rosta, N. J. Russ, N. Sergueev, S. M. Sharada, S. Sharmaa, D. W. Small, A. Sodt, T. Stein, D. Stück, Y.-C. Su, A. J. W. Thom, T. Tsuchimochi, L. Vogt, O. Vydrov, T. Wang, M. A. Watson, J. Wenzel, A. White, C. F. Williams, V. Vanovschi, S. Yeganeh, S. R. Yost, Z.-Q. You, I. Y. Zhang, X. Zhang, Y. Zhou, B. R. Brooks, G. K. L. Chan, D. M. Chipman, C. J. Cramer, W. A. Goddard III, M. S. Gordon, W. J. Hehre, A. Klamt, H. F. Schaefer III, M. W. Schmidt, C. D. Sherrill, D. G. Truhlar, A. Warshel, X. Xua, A. Aspuru-Guzik, R. Baer, A. T. Bell, N. A. Besley, J.-D. Chai, A. Dreuw, B. D. Dunietz, T. R. Furlani, S. R. Gwaltney, C.-P. Hsu, Y. Jung, J. Kong, D. S. Lambrecht, W. Liang, C. Ochsenfeld, V. A. Rassolov, L. V. Slipchenko, J. E. Subotnik, T. Van Voorhis, J. M. Herbert, A. I. Krylov, P. M. W. Gill, and M. Head-Gordon, Mol. Phys. **113**, 184 (2015).
[45]See supplementary material at http://dx.doi.org/10.1063/1.4926837 for Cartesian coordinates of the molecular complexes examined herein.
[46]A. Lange and J. M. Herbert, J. Chem. Theory Comput. **3**, 1680 (2007).
[47]E. J. Baerends, O. V. Gritsenko, and R. van Meer, Phys. Chem. Chem. Phys. **15**, 16408 (2013).
[48]R. van Meer, O. V. Gritsenko, and E. J. Baerends, J. Chem. Theory Comput. **10**, 4432 (2014).
[49]J. Kim, K. Hong, S. Choi, S.-Y. Hwang, and W. Y. Kim, Phys. Chem. Chem. Phys. (in press).
[50]Y. Chen and H. Li, J. Phys. Chem. A **114**, 11719 (2010).
[51]J. K. Kazimirski and V. Buch, J. Phys. Chem. A **107**, 9762 (2003).
[52]M. Head-Gordon, A. M. Graña, D. Maurice, and C. A. White, J. Phys. Chem. **99**, 14261 (1995).
[53]H. Shao, J. Seifert, N. C. Romano, M. Gao, J. J. Helmus, C. P. Jaroniec, D. A. Modarelli, and J. R. Parquette, Angew. Chem., Int. Ed. Engl. **49**, 7688 (2010).
[54]H. Shao, M. Gao, S. H. Kim, C. P. Jaroniec, and J. R. Parquette, Chem. - Eur. J. **17**, 12882 (2011).
[55]M. A. Rohrdanz, K. M. Martins, and J. M. Herbert, J. Chem. Phys. **130**, 054112 (2009).
[56]A. F. Morrison and J. M. Herbert, "A low-order scaling approach to excited-state properties based on an *ab initio* exciton model with charge embedding" (unpublished).
[57]See http://osc.edu/ark:/19495/f5s1ph73 for Ohio Supercomputer Center.